

Preparation and Properties of Tetrathia- and Tetramethyl-tetraselena-fulvalene Salts of $[M_6O_{19}]^{2-}$ ($M = Mo$ or W)[†]

Smail Triki,^a Lahcène Ouahab,^{*a} Jean-François Halet,^{*a} Octavio Pena,^a Jean Padiou,^a Daniel Grandjean,^a Chantal Garrigou-Lagrange^b and Pierre Delhaes^{*b}

^a *Laboratoire de Chimie du Solide et Inorganique Moléculaire, U.R.A. 254 CNRS, Université de Rennes I, 35042 Rennes Cedex, France*

^b *Centre de Recherche Paul Pascal, CNRS, Avenue Albert Schweitzer, 33600 Pessac, France*

The preparation, X-ray crystal structures, conductivity and optical properties of the salts, $[tff]_3[W_6O_{19}]$ **1**, $[tff]_3[Mo_6O_{19}]$ **2** (tff = tetrathiafulvalene) and $[tmtsf]_3[W_6O_{19}] \cdot 2dmf$ **3** (tmtsf = tetramethyltetraselenafulvalene) are reported. Crystal data: **1**, triclinic, space group $P\bar{1}$, $a = 9.965(3)$, $b = 10.503(3)$, $c = 10.634(3)$ Å, $\alpha = 71.93(2)$, $\beta = 78.63(2)$, $\gamma = 63.38(3)$, $Z = 1$, $R = 0.020$; **2**, triclinic, space group $P\bar{1}$, $a = 9.942(3)$, $b = 10.417(3)$, $c = 10.601(3)$, $\alpha = 72.33(2)$, $\beta = 78.77(2)$, $\gamma = 63.52(3)^\circ$, $Z = 1$, $R = 0.030$; **3**, monoclinic, space group $P2_1/c$, $a = 11.589(4)$, $b = 19.385(5)$, $c = 13.681(3)$, $\beta = 99.53(2)$, $Z = 2$ and $R = 0.049$. In all the salts the organic molecules form trimerized stacks. A classical ring-over-double bond overlap is observed in **3**, in contrast with **1** and **2** which present an unusual intra-trimer criss-cross overlap. In compound **3** the intra-trimer Se...Se (3.73–3.81 Å) contacts are shorter than those observed in $[tmtsf]_2X$ ($X = PF_6$ or BF_4) series. The inter-trimer Se...Se contacts (3.94–4.12 Å) are in the range of the van der Waals separation (4 Å). Short O...Se (3.17–3.30 Å) contacts are observed. Both electrical and optical measurements and also electronic band-structure calculations reveal that the three salts are semiconductors.

We are currently studying the charge-transfer complexes arising from organic donors derived from the tetrathia(selena)fulvalenes and inorganic anions which have specific properties. Our goal is to obtain new materials containing organic and inorganic blocks in the mixed-valence states.^{1–3} In this work the inorganic counterparts that are chosen are the polyoxometalate dianions $[M_6O_{19}]^{2-}$ ($M = W$ or Mo) which result from the condensation of six MO_6 octahedra sharing common vertices and adopt the so-called Lindquist structure.^{4a} Known for over a century, the polyoxometalates are still of interest because of their high electron-acceptor ability.⁵ The presence of inorganic acceptor anions in charge-transfer salts can induce the co-existence of mixed-valence states in the organic and inorganic systems. The stabilization of such a mixed-valence state is one of the prerequisite conditions for electron delocalization (electrical conductivity) or unpaired spin localization on the transition metal d orbitals (magnetic properties). Since our first attempt^{1,2a} to synthesise new adducts combining tetrathiafulvalene derivatives and α -Keggin^{4b} phosphotungstate or Lindquist^{4a} hexametallate polyanions several other organic-inorganic salts have been characterized in our laboratory³ and by Bellito *et al.*^{2b} Following a preliminary note,^{2a} we report here in detail the preparation, X-ray crystal structure, conductivity, magnetic and spectroscopic characterizations of $[tff]_3[W_6O_{19}]$ **1**, $[tff]_3[Mo_6O_{19}]$ **2** and $[tmtsf]_3[W_6O_{19}] \cdot 2dmf$ **3** {tff = tetrathiafulvalene [2-(1',3'-dithiol-2'-ylidene)-1,3-dithiole], tmtsf = tetramethyltetraselenafulvalene [2-(4',5'-dimethyl-1',3'-diselenol-2'-ylidene)-4,5-dimethyl-1,3-diselenole] and dmf = dimethylformamide}.

Experimental

Preparations.—The compounds tff and tmtsf (Fluka) were used as received. Acetonitrile, dichloromethane and dimethyl-

formamide (Fluka) were distilled and passed through activated neutral alumina before use. The compounds $[NET_4]_2[Mo_6O_{19}]$, $[NBu_4]_2[Mo_6O_{19}]$ and $[NBu_4]_2[W_6O_{19}]$ were prepared and recrystallized according to refs. 6 and 7. Their stoichiometries were determined by elemental analysis [Calc. (Found) for $[NET_4]_2[Mo_6O_{19}] \cdot 2H_2O$: C, 16.35 (16.40); H, 3.75 (3.90); Mo, 48.93 (48.75); N, 2.40 (2.30). For $[NBu_4]_2[Mo_6O_{19}]$: C, 28.15 (28.40); H, 5.30 (5.35); Mo, 42.20 (43.25); N, 2.05 (2.05). For $[NBu_4]_2[W_6O_{19}]$: C, 20.30 (20.70); H, 3.80 (4.10); N, 1.50 (1.35); W, 58.35 (54.65)%]. The electrocrystallizations were carried out in a U-shaped cell (25 cm³) with the two electrolytic compartments separated by glass frits (porosity 3). The electrodes comprised platinum wire (diameter 1 mm) immersed in the degassed solution to a depth of 2.5 cm. The constant current was stabilized by a regulator made in our laboratory.

$[tff]_3[W_6O_{19}]$ **1** and $[tff]_3[Mo_6O_{19}]$ **2**. Anodic oxidation of the organic donor tff (2×10^{-3} mol dm⁻³) at a low constant current ($I = 1 \mu A$) in the presence of the tetraalkylammonium salt of the $[M_6O_{19}]^{2-}$ dianion (10^{-2} mol dm⁻³) as supporting electrolyte in acetonitrile led to polyhedral block-shaped black crystals after several weeks. The stoichiometries were determined unambiguously by X-ray crystal structure analysis. The two compounds can be obtained either with $[NBu_4]_2[M_6O_{19}]$ or $[NET_4]_2[M_6O_{19}]$ as supporting electrolyte.

$[tmtsf]_3[W_6O_{19}] \cdot 2dmf$ **3**. The anodic oxidation of tmtsf (2×10^{-3} mol dm⁻³) at a low constant current ($I = 1.25 \mu A$) in the presence of $[NBu_4]_2[W_6O_{19}]$ (10^{-2} mol dm⁻³) as supporting electrolyte led to black needle crystals with hexagonal sections (1–2 mm long) after 1 week. A mixture of dmf and CH_2Cl_2 (ratio 3:1) was used [Calc. (Found) for $C_{36}H_{50}N_2O_{21}Se_{12}W_6$: C, 14.90 (15.15); H, 1.70 (1.55); N, 0.95 (0.90); Se, 32.70 (33.20); W, 38.05 (37.65)%]. Attempts to prepare the corresponding $[Mo_6O_{19}]^{2-}$ salt under the same experimental conditions failed.

X-Ray Crystal Structure Analysis.—Black crystals of compounds **1–3** were mounted on an Enraf-Nonius CAD4 diffractometer equipped with graphite-crystal-monochromatized

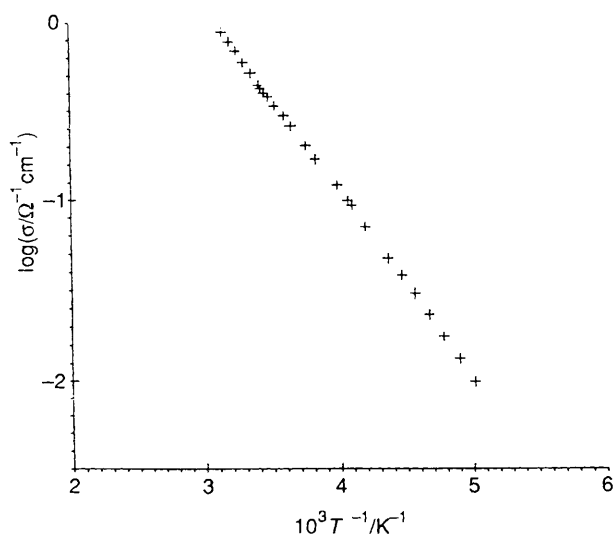
[†] Supplementary data available: see Instructions for Authors, *J. Chem. Soc., Dalton Trans.*, 1992, Issue 1, pp. xx–xxv.

Non-SI units employed: eV $\approx 1.60 \times 10^{-19}$ J, Oe = 10^3 A m⁻¹.

Table 1 Crystal and refinement data for compounds 1–3

| Compound | [tff] ₃ [W ₆ O ₁₉] 1 | [tff] ₃ [Mo ₆ O ₁₉] 2 | [tmfsf] ₃ [W ₆ O ₁₉]·2dmf 3 |
|---|--|---|--|
| <i>(a) Crystal data</i> | | | |
| Formula | C ₁₈ H ₁₂ O ₁₉ S ₁₂ W ₆ | C ₁₈ H ₁₂ Mo ₆ O ₁₉ S ₁₂ | C ₃₆ H ₅₀ N ₂ O ₂₁ Se ₁₂ W ₆ |
| <i>M</i> | 2020.15 | 1492.69 | 2897.42 |
| Crystal system | Triclinic | Triclinic | Monoclinic |
| Space group | <i>P</i> $\bar{1}$ | <i>P</i> $\bar{1}$ | <i>P</i> 2 ₁ / <i>c</i> |
| <i>a</i> /Å | 9.965(3) | 9.942(3) | 11.589(4) |
| <i>b</i> /Å | 10.503(3) | 10.417(3) | 19.385(5) |
| <i>c</i> /Å | 10.634(3) | 10.601(3) | 13.681(3) |
| α /° | 71.93(2) | 72.33(2) | 90 |
| β /° | 78.63(2) | 78.77(2) | 99.53(2) |
| γ /° | 63.38(3) | 63.52(3) | 90 |
| <i>U</i> /Å ³ | 943.8 | 933.9 | 3030.9 |
| <i>Z</i> | 1 | 1 | 2 |
| <i>D</i> _c /g cm ⁻³ | 3.554 | 2.654 | 3.175 |
| <i>F</i> (000) | 908 | 716 | 2600 |
| <i>(b) Data collection and refinement parameters</i> | | | |
| Crystal size/mm | 0.3 × 0.1 × 0.1 | 0.15 × 0.15 × 0.1 | 0.35 × 0.1 × 0.1 |
| μ (Mo-K α)/cm ⁻¹ | 193.23 | 26.29 | 187.94 |
| <i>h, k, l</i> Ranges | 0–13, –13 to 13, –14 to 14 | –13 to 13, –13 to 13, 0–14 | 0–13, 0–23, –16 to 16 |
| 2 θ Limits/° | 2–50 | 2–50 | 2–50 |
| No. of reflections: | | | |
| unique | 3361 | 4244 | 5045 |
| [<i>F</i> _o ≥ <i>n</i> σ (<i>F</i> _o)] | 3380, <i>n</i> = 3 | 2729, <i>n</i> = 6 | 2294, <i>n</i> = 3 |
| <i>R</i> _{int} | 0.047 | 0.013 | 0.026 |
| No. variables | 251 | 251 | 310 |
| <i>R</i> (<i>F</i>), ^a <i>R</i> '(<i>F</i>) ^b | 0.020, 0.030 | 0.030, 0.046 | 0.049, 0.063 |
| <i>S</i> ^c | 0.739 | 1.118 | 1.314 |
| Δ/σ | 0.10 | 0.01 | 11.61 |
| $\Delta\rho/e$ Å ⁻³ | 1.179 | 1.616 | 2.712 |

^a $R = \Sigma[|F_o| - |F_c|]/\Sigma|F_o|$. ^b $R' = [\Sigma w(|F_o| - |F_c|)^2/\Sigma w|F_o|^2]^{1/2}$, where $w = 4F_o^2/[\sigma^2(I) + (0.07|F_o|^2)^2]$. ^cGoodness of fit (*s*) = $[\Sigma w(|F_o| - |F_c|)^2/(N_{obs} - N_{var})]^{1/2}$.

**Fig. 1** The d.c. conductivity of [tmfsf]₃[W₃O₁₉]·2dmf

Mo-K α radiation ($\lambda = 0.71073$ Å). The cell dimensions have been determined and refined by the least-squares method from setting angles of 25 centred reflections. The intensities were collected by θ – 2θ scans. Three standard reflections measured every hour revealed no fluctuations in intensities. One set of reflections were collected up to $2\theta = 50^\circ$. Lorentz, polarization and absorption corrections were applied. The absorption corrections were performed using the ψ -scan^{8a} method for compounds 1 and 3 and the DIFABS procedure^{8b} for 2. Crystal data are summarized in Table 1.

The structures were solved by direct methods (MULTAN

84)⁹ and successive Fourier difference syntheses. Every structure was refined by weighted anisotropic full-matrix least-squares methods. After refinement of positional and anisotropic (β_{ij}) thermal parameters for all non-hydrogen atoms, the positions of the H atoms were calculated [$d(C-H) = 1$ Å; $B_{eq} = 4$ Å²] and included as a fixed contribution to F_c . In compound 3 the atoms of the dmf molecule and O(4), C(1) and C(6) were refined isotropically. Scattering factors and corrections for anomalous dispersion were taken from ref. 10. The molecular and crystal structure illustrations were drawn with ORTEP.¹¹ All the calculations were performed on a PDP11/60 computer using the SDP programs described by Frenz.¹² The positional atomic coordinates are given in Table 2, bond lengths and angles in Table 3 (see also Figs. 5 and 11).

Additional material available from the Cambridge Crystallographic Data Centre comprises H-atom coordinates, thermal parameters and remaining bond lengths and angles.

Electrical Conductivity.—The d.c. electrical conductivities were measured by use of a standard four-probe technique. All salts 1–3 are semiconducting with absolute room-temperature values (σ_{300K}) equal to 1.4×10^{-3} , 0.5×10^{-3} and $1.3 \Omega^{-1} \text{cm}^{-1}$, respectively. The temperature dependence of the single-crystal d.c. electrical conductivity along the needle axis is presented in Fig. 1 for 3 and yields an activation energy of 0.2 eV.

Optical Properties.—An IR Nicolet MX1 interferometer (350 – 4800 cm^{-1}) and a UV/VIS Perkin-Elmer 350 spectrometer (3850 – $25\,000 \text{ cm}^{-1}$) were used for comparative transmission measurements of finely ground KBr pellet samples. The IR spectra were recorded at different temperatures down to 15 K with a ⁴He cryostat.

The electronic spectra of the three salts are illustrated in Fig. 2, except the vibrational bands, observed at lower frequencies.

Table 2 Atomic coordinates with standard deviations

| Atom | X/a | Y/b | Z/c | Atom | X/a | Y/b | Z/c |
|--|--------------|--------------|--------------|----------------------|------------|-------------|------------|
| <i>(a)</i> [ttf] ₃ [W ₆ O ₁₉] | | | | | | | |
| The anion | | | | ttf/A | | | |
| W(1) | -0.253 36(2) | 0.160 98(2) | -0.001 32(2) | S(1) | 0.736 8(2) | 0.352 2(2) | 0.497 1(2) |
| W(2) | 0.015 56(2) | 0.052 13(2) | -0.230 03(2) | S(2) | 0.541 3(2) | 0.553 0(2) | 0.286 2(2) |
| W(3) | -0.062 89(2) | -0.193 33(2) | 0.014 38(2) | C(1) | 0.559 2(6) | 0.481 6(6) | 0.453 1(5) |
| O(1) | -0.439 2(5) | 0.278 8(6) | -0.002 4(4) | C(2) | 0.813 1(7) | 0.359 2(7) | 0.335 9(7) |
| O(2) | -0.024 8(5) | -0.091 0(5) | 0.398 3(4) | C(3) | 0.725 6(8) | 0.449 1(7) | 0.241 1(7) |
| O(3) | 0.107 4(6) | 0.335 9(5) | -0.025 7(6) | ttf/B | | | |
| O(4) | -0.214 9(4) | 0.087 2(5) | 0.185 1(4) | S(3) | 0.175 3(2) | 0.371 5(2) | 0.466 5(2) |
| O(5) | -0.192 1(4) | 0.170 4(4) | -0.184 2(4) | S(4) | 0.430 8(2) | 0.299 2(2) | 0.272 2(2) |
| O(6) | -0.153 9(5) | 0.284 4(4) | -0.011 2(4) | S(5) | 0.649 9(2) | 0.080 3(2) | 0.502 9(2) |
| O(7) | -0.252 9(4) | -0.028 0(4) | 0.012 5(4) | S(6) | 0.400 8(2) | 0.156 7(2) | 0.701 9(2) |
| O(8) | 0.059 2(4) | 0.199 3(4) | -0.196 0(4) | C(4) | 0.367 2(6) | 0.274 4(6) | 0.437 8(6) |
| O(9) | 0.037 3(4) | 0.114 3(4) | 0.172 7(4) | C(5) | 0.139 8(8) | 0.436 5(8) | 0.300 7(8) |
| O(10) | 0 | 0 | 0 | C(6) | 0.256 0(8) | 0.402 0(8) | 0.212 6(7) |
| <i>(b)</i> [ttf] ₃ [Mo ₆ O ₁₉] | | | | | | | |
| The anion | | | | ttf/A | | | |
| Mo(1) | 0.252 87(5) | -0.162 80(5) | 0.005 10(5) | S(1) | 0.737 8(2) | 0.352 1(2) | 0.499 1(2) |
| Mo(2) | 0.020 23(5) | 0.049 27(5) | -0.229 86(4) | S(2) | 0.542 9(2) | 0.551 0(2) | 0.285 7(1) |
| Mo(3) | -0.063 85(5) | -0.191 84(5) | 0.013 67(5) | C(1) | 0.561 0(6) | 0.479 1(5) | 0.453 7(5) |
| O(1) | 0.437 2(4) | -0.275 9(5) | 0.003 0(4) | C(2) | 0.814 0(7) | 0.354 5(6) | 0.340 7(7) |
| O(2) | 0.027 4(4) | 0.087 1(4) | -0.395 1(4) | C(3) | 0.726 8(8) | 0.446 3(7) | 0.239 8(7) |
| O(3) | -0.105 1(5) | -0.334 8(4) | 0.024 2(5) | ttf/B | | | |
| O(4) | 0.215 6(4) | -0.085 3(4) | -0.186 6(3) | S(3) | 0.174 2(2) | 0.370 8(2) | 0.465 4(2) |
| O(5) | 0.194 4(4) | -0.167 9(4) | 0.184 6(4) | S(4) | 0.432 0(2) | 0.297 6(2) | 0.272 2(1) |
| O(6) | 0.157 1(4) | -0.285 1(4) | 0.008 7(4) | S(5) | 0.649 0(2) | 0.079 6(2) | 0.506 7(2) |
| O(7) | 0.253 7(4) | 0.030 1(4) | -0.016 0(4) | S(6) | 0.395 6(2) | 0.158 7(2) | 0.702 7(2) |
| O(8) | 0.054 2(4) | 0.201 4(4) | -0.196 8(4) | C(4) | 0.366 0(5) | 0.274 1(5) | 0.436 2(5) |
| O(9) | -0.038 9(4) | -0.115 5(4) | -0.173 8(4) | C(5) | 0.143 0(7) | 0.437 8(7) | 0.299 7(8) |
| O(10) | 0 | 0 | 0 | C(6) | 0.257 2(8) | 0.402 5(7) | 0.211 6(7) |
| <i>(c)</i> [tmtsf] ₃ [W ₆ O ₁₉]-2dmf | | | | | | | |
| The anion | | | | tmtsf/B | | | |
| W(1) | 0.126 7(1) | 0.057 61(6) | -0.087 16(9) | Se(3) | 0.289 7(3) | 0.072 9(2) | 0.629 2(2) |
| W(2) | 0.032 1(1) | 0.083 58(6) | 0.123 20(9) | Se(4) | 0.243 3(3) | 0.095 0(2) | 0.397 7(2) |
| W(3) | 0.156 0(1) | -0.063 70(6) | 0.082 64(8) | Se(5) | 0.406 4(3) | -0.086 0(2) | 0.593 7(2) |
| O(1) | 0.218(2) | 0.099(1) | -0.150(2) | Se(6) | 0.354 3(3) | -0.060 1(2) | 0.364 0(2) |
| O(2) | -0.059(2) | -0.147(1) | -0.211(1) | C(6)* | 0.303(2) | 0.040(1) | 0.501(2) |
| O(3) | 0.267(2) | 0.110(1) | 0.143(1) | C(7) | 0.234(2) | 0.158(1) | 0.577(2) |
| O(4)* | 0.080(1) | -0.021 1(9) | -0.168(1) | C(8) | 0.213(3) | 0.169(1) | 0.480(2) |
| O(5) | 0.127(2) | 0.113 8(9) | 0.027(1) | C(9) | 0.211(3) | 0.215(2) | 0.653(2) |
| O(6) | 0.223(2) | -0.005 6(9) | -0.002(1) | C(10) | 0.172(3) | 0.235(2) | 0.420(3) |
| O(7) | -0.025(2) | 0.099 8(9) | -0.139(1) | C(11) | 0.349(3) | -0.025(1) | 0.491(2) |
| O(8) | 0.100(1) | -0.116 8 | -0.032(1) | C(12) | 0.437(3) | -0.157(2) | 0.502(3) |
| O(9) | 0.154(2) | 0.013 8(9) | 0.165(1) | C(13) | 0.415(3) | -0.145(2) | 0.406(2) |
| O(10) | 0 | 0 | 0 | C(14) | 0.491(4) | -0.219(1) | 0.560(3) |
| tmtsf/A | | | | C(15) | 0.448(3) | -0.193(2) | 0.329(3) |
| Se(1) | -0.034 3(3) | 0.069 9(1) | 0.628 7(2) | dmf solvent molecule | | | |
| Se(2) | -0.079 7(3) | 0.087 9(2) | 0.397 5(2) | N* | 0.539(3) | 0.431(2) | 0.644(3) |
| C(1)* | -0.022(2) | 0.032(1) | 0.505(2) | O(1a)* | 0.487(2) | 0.441(1) | 0.416(2) |
| C(2) | -0.094(3) | 0.155(1) | 0.579(2) | O(16)* | 0.413(3) | 0.404(2) | 0.635(2) |
| C(3) | -0.111(3) | 0.161(1) | 0.480(2) | O(17)* | 0.633(3) | 0.401(2) | 0.636(2) |
| C(4) | -0.119(3) | 0.209(2) | 0.649(2) | O(18)* | 0.472(3) | 0.496(2) | 0.361(3) |
| C(5) | -0.165(3) | 0.224(2) | 0.419(3) | | | | |

* Atoms refined isotropically

We note the presence of both the 'A' and 'B' charge-transfer (c.t.) bands (Torrance's notation,¹³ respectively around 6000 and

12 500 cm⁻¹ for the ttf salts and around 3800 and 12 000 cm⁻¹ for the tmtsf salts. The observed frequencies for the 'A' bands

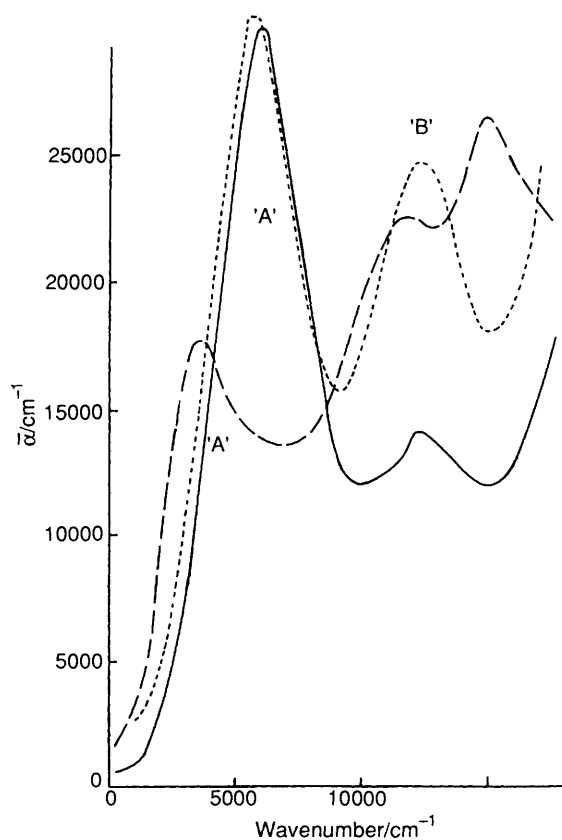


Fig. 2 Plots of the mean electronic absorption coefficient (\bar{x} in cm^{-1}) determined for KBr pellets at room temperature versus the energy (in wavenumbers) for $[\text{ttf}]_3[\text{W}_6\text{O}_{19}]$ (—), $[\text{ttf}]_3[\text{Mo}_6\text{O}_{19}]$ (····) and $[\text{tmtsf}]_3[\text{W}_6\text{O}_{19}] \cdot 2\text{dmf}$ (-----)

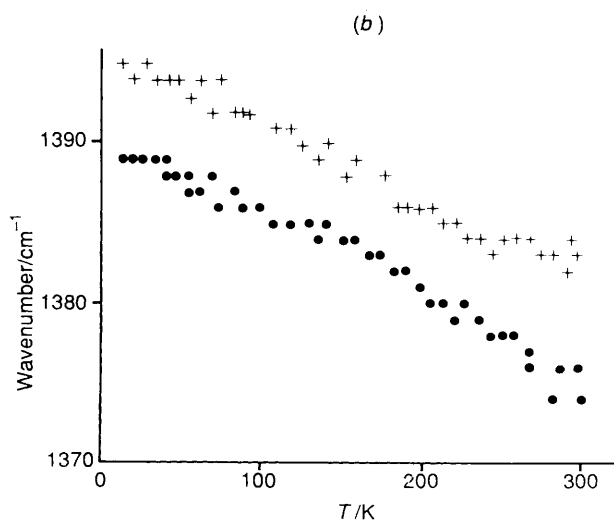
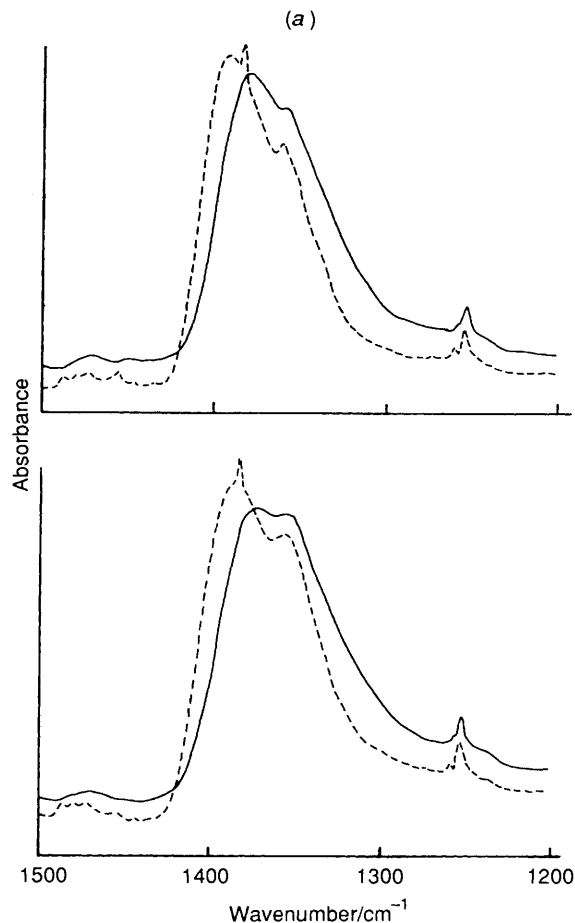


Fig. 4 (a) Infrared spectra between 1500 and 1200 cm^{-1} of $[\text{ttf}]_3[\text{W}_6\text{O}_{19}]$ (upper) and $[\text{ttf}]_3[\text{Mo}_6\text{O}_{19}]$ (lower) at 15 (-----) and 300 K (—). (b) Temperature dependence of the vibronic band frequency $a_g v(\text{C}=\text{C})$ for $[\text{ttf}]_3[\text{W}_6\text{O}_{19}]$ (+) and $[\text{ttf}]_3[\text{Mo}_6\text{O}_{19}]$ (●)

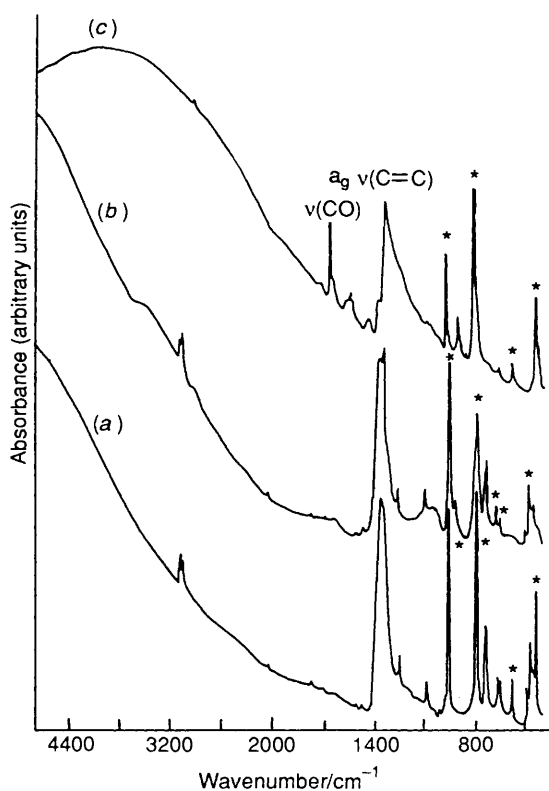
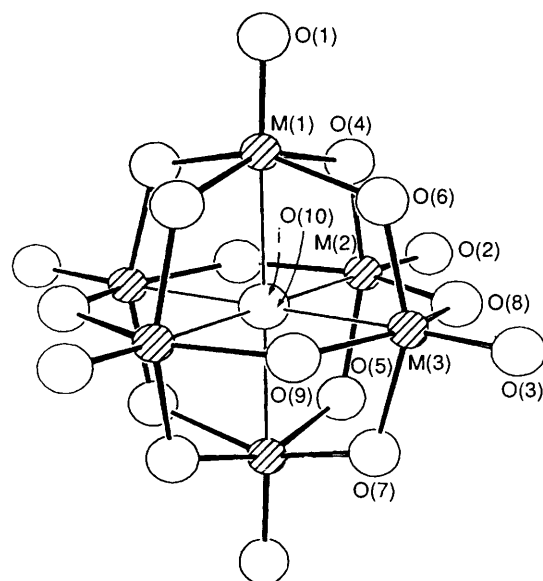


Fig. 3 Infrared absorption spectra between 4800 and 400 cm^{-1} of (a) $[\text{ttf}]_3[\text{W}_6\text{O}_{19}]$, (b) $[\text{ttf}]_3[\text{Mo}_6\text{O}_{19}]$ and (c) $[\text{tmtsf}]_3[\text{W}_6\text{O}_{19}] \cdot 2\text{dmf}$ at room temperature (the anion bands are labelled with asterisks)

are almost identical to those observed for $[\text{tmtsf}]_3[\text{M}(\text{CN})_4]$ ($\text{M} = \text{Pt}$ or Ni)¹⁴⁻¹⁶ or $[\text{ttf}]_{14}[\text{MCl}_4]_4$ ($\text{M} = \text{Mn}$ or Co) salts:¹⁷ they are characteristic of a mixed-valence state. So far, however, we have not observed simultaneously the 'A' and 'B' bands in the absorption spectra of ttf and tmtsf salts.

From Fig. 3, showing the room-temperature infrared spectra of our three Lindquist salts, we can immediately recognize the $\nu(\text{C}=\text{O})$ band of the solvent molecule (dmf) present in the crystal structure of $[\text{tmtsf}]_3[\text{W}_6\text{O}_{19}] \cdot 2\text{dmf}$ and the characteristic bands of the $[\text{W}_6\text{O}_{19}]^{2-}$ and $[\text{Mo}_6\text{O}_{19}]^{2-}$ dianions.



Scheme 1

These bands have been attributed by comparison with literature data.¹⁸ Fig. 4(a) presents the expanded region between 1500 and 1200 cm^{-1} at room temperature and at 15 K for the two ttf salts **1** and **2**. The lower band situated around 1355 cm^{-1} whose frequency does not vary with temperature is probably due to a combination of the F_{1u} and A_g vibrations of the anions at around 880 and 600 cm^{-1} respectively.¹⁸ On the other hand, the wavenumber of the other component of the doublet is 15 cm^{-1} higher at 15 K than at room temperature. This band is due to the vibronic a_g $\nu(\text{C}=\text{C})$ vibration.¹⁷ Its temperature dependence is also given in Fig. 4(b).

The $\nu(\text{C}=\text{C})$ a_g band of the tmtsf salt **3** is observed around 1335 cm^{-1} and its frequency does not vary with temperature. Therefore, we can assume that no structural phase transition occurs for this salt.

Magnetic Susceptibility.—Magnetic susceptibility measurements were performed in the range $2 \leq T \leq 300$ K using a variable-temperature SQUID susceptometer (SHE-VTS-906) under a magnetic field strength of 1 or 5 kOe. An almost constant diamagnetic signal was observed over the whole temperature range. In order to get a more precise estimation of the diamagnetic contribution of the compounds, additional measurements were performed at fixed temperatures (300 and 100 K) at 20 and 50 kOe, yielding diamagnetic contributions of 9.32×10^{-9} , 4.57×10^{-9} and 4.26×10^{-9} $\text{m}^3 \text{kg}^{-1} \text{mol}^{-1}$ at room temperature for salts **1**, **2** and **3** respectively. Such values are in reasonable agreement with the total diamagnetic contributions calculated using Pascal's tables.

Electronic Band-structure Calculations.—All molecular and solid tight-binding¹⁹ calculations were carried out within the extended-Hückel formalism²⁰ using standard atomic parameters for H, C, S and Se. The exponent (ζ) and the valence-shell ionization potential (H_{ii} in eV) were respectively: 1.3, -13.6 for H 1s; 1.625, -21.4 for C 2s; 1.625, -11.4 for C 2p; 1.817, -20.0 for S 3s; 1.817, -13.3 for S 3p; 2.44, -20.5 for Se 4s and 2.07, -13.2 for Se 4p. A set of 8k points, chosen in the irreducible part of the oblique Brillouin zone, according to the Ramirez and Bohm method²¹ was used to calculate the atomic charges of the organic (ttf)₃ slab present in **1** and **2**. The symbols Γ , X and Y refer to points of the Brillouin zone of coordinates (0, 0), ($a^*/2$, 0) and (0, $b^*/2$) respectively. A set of 9k points was used to calculate the atomic charges of the organic (tmtsf)₃ chain encountered in **3**. For computational reasons, the methyl groups of the tmtsf molecules were replaced by hydrogen atoms.

Results and Discussion

Description of the $\text{M}_6\text{O}_{19}^{2-}$ Anions.—The structure of the $[\text{M}_6\text{O}_{19}]^{2-}$ anions (Scheme 1) consists of a central oxygen atom O_c [e.g. O(10)] surrounded octahedrally by six metal atoms which are bonded through oxygen bridges O_b [e.g. O(4)]. One terminal oxygen atom O_t [e.g. O(1)] is bonded to each metal. The structure can be described as a condensation of six distorted MO_6 octahedra sharing common vertices at the central oxygen atom. Each MO_6 octahedron has common edges with four neighbouring ones. The bond distances and angles are given in Table 2. In the $[\text{W}_6\text{O}_{19}]^{2-}$ units the average bond distances observed in **1** and **3** [W-W 3.292, 3.286; W- O_t 1.705(5), 1.68(2); W- O_b 1.924(5), 1.92(2); and W- O_c 2.328(1), 2.323(1) Å] are in good agreement and compare well with the corresponding ones found as in $[\text{NBu}_4]_2[\text{W}_6\text{O}_{19}]^{22a}$ or $[\text{N}(\text{PPh}_3)_2]_2[\text{W}_6\text{O}_{19}]^{22b}$. In the Mo_6O_{19} unit (compound **2**) the average Mo-Mo (3.277 Å), Mo- O_t [1.678(5) Å], Mo- O_b [1.924(4) Å] and Mo- O_c [2.317(1) Å] bond distances are close to the corresponding ones found, for instance, in $[\text{HN}_3\text{P}_3(\text{NMe}_2)_6]_2[\text{Mo}_6\text{O}_{19}]^{23a}$ or $[\text{AsPh}_4]_2[\text{Mo}_6\text{O}_{19}]^{23b}$.

$[\text{ttf}]_3[\text{W}_6\text{O}_{19}]$ **1 and $[\text{ttf}]_3[\text{Mo}_6\text{O}_{19}]$ **2**.**—**Crystal structures.** The bond distances and angles are given in Fig. 5 for the ttf molecules of $[\text{ttf}]_3[\text{W}_6\text{O}_{19}]$ **1** and $[\text{ttf}]_3[\text{Mo}_6\text{O}_{19}]$ **2**. Both salts are isostructural. The crystal structures represented in Figs. 6 and 7 are built from $[\text{W}_6\text{O}_{19}]^{2-}$ or $[\text{Mo}_6\text{O}_{19}]^{2-}$ anions located at the origin of the lattice, and two independent ttf units denoted A and B: one (A) positioned on the $(\frac{1}{2}, \frac{1}{2}, \frac{1}{2})$ inversion centre and the other (B) in general position.

The bond distances of the two independent ttf molecules in both compounds **1** and **2** are averaged in the *mm* symmetry and compared in Table 4 with the corresponding distances in ttf^{x+} salts ($x = 0$ or 1).²⁴⁻²⁸ We note a slight difference in the C-C and S-C bond distances between the A and B ttf molecules for compounds **1** and **2**. Molecules A and B form a stack of trimers with a BAB-BAB sequence (Fig. 6). The overlap between successive trimers, *i.e.* between the molecule B and its centrosymmetry-related one can be described as a ring-over-double bond overlap followed by a transversal displacement.^{2a} The intra-trimer overlap, *i.e.* between molecules A and B, is of criss-cross type with an eclipse angle of 90° (Fig. 7). This mode of overlap has been observed for instance in $[\text{tmtsf}][\text{FeCl}_4]$ and its sulfur analogues,²⁹ $[\text{tmtsf}][\text{ReO}_4] \cdot 0.25\text{C}_2\text{H}_3\text{Cl}_3$ ³⁰ and $[\text{tmtsf}]_3[\text{PW}_{12}\text{O}_{40}]$.³ Such a packing leads to strong intra-trimer S...S interactions (Fig. 6). The intertrimer S...S contacts are longer than the van der Waals separation of 3.8 Å. Additionally, there are short anion-cation S...O and inter-chain S...S contacts (Figs. 6 and 8).

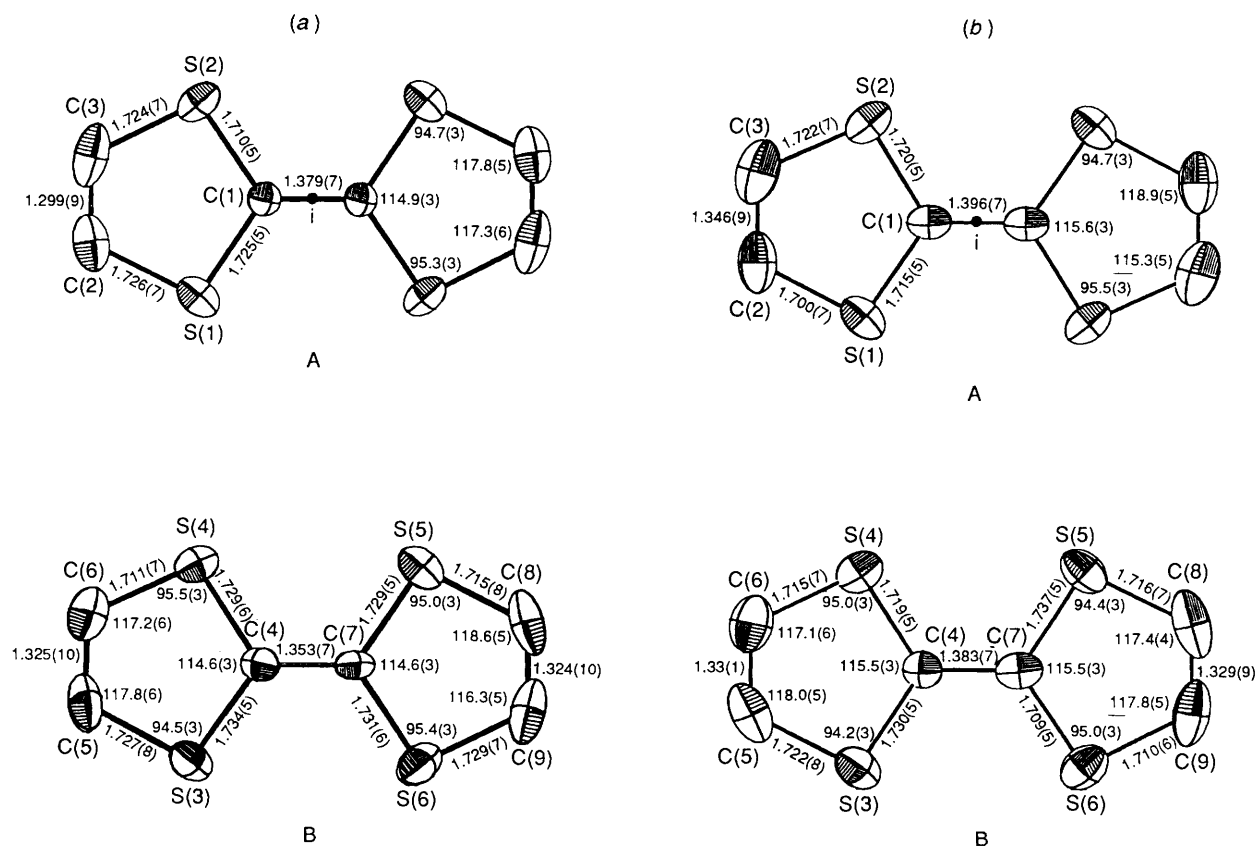
Theoretical band calculations. A pertinent question is the assignment of the oxidation state of the ttf molecules constituting the organic (ttf)₃²⁺ stack in $[\text{ttf}]_3[\text{W}_6\text{O}_{19}]$ **1** and $[\text{ttf}]_3[\text{Mo}_6\text{O}_{19}]$ **2**. Is there a mixed-valence $\text{ttf}^{\frac{1}{3}+}$, ttf^+ , $\text{ttf}^{\frac{2}{3}+}$ structure, corresponding to inequivalent sites, or a statistical $\text{ttf}^{\frac{1}{3}+}$, ttf^+ , $\text{ttf}^{\frac{2}{3}+}$ one for equivalent sites in compounds **1** and **2**? In order to elucidate this point we performed tight-binding calculations within the extended-Hückel formalism on the two-dimensional organic sublattice (ttf)₃²⁺ present in **1** and **2** (see Fig. 8).

Since the (ttf)₃²⁺ chains in this sublattice are constructed from the stacking of nearly isolated criss-cross (ttf)₃²⁺ trimers (see above), the natural starting point is to look at the bonding features of an idealized pseudo-molecular (ttf)₃²⁺ model **a** of symmetry D_{2h} , made of two 'outside' ttf molecules (B and B') and an 'inside' one (A). Identical central C-C, C-S and edge C-C bond distances (Å) of 1.35, 1.72 and 1.313 respectively were taken for all of them. Consideration only of the highest occupied molecular orbital (HOMO) of the neutral ttf molecule is generally sufficient to discuss the factors affecting the electronic and structural properties of organic salts.³¹

The HOMO of ttf is concentrated heavily on the p_π atomic orbitals of the S and central C atoms.³² Being bonding between

Table 3 Bond distances (Å) and selected bond angles (°) in the $M_6O_{19}^{2-}$ units (see Scheme 1 for labelling)

| | 1 (M = W) | 2 (M = Mo) | 3 (M = W) | | 1 (M = W) | 2 (M = Mo) | 3 (M = W) |
|-----------------|-----------|------------|-----------|-----------------|-----------|------------|-----------|
| M(1)–O(1) | 1.705(4) | 1.680(4) | 1.67(2) | M(2)–O(8) | 1.929(5) | 1.900(5) | 1.92(2) |
| M(1)–O(4) | 1.939(4) | 1.987(4) | 1.91(2) | M(2)–O(9) | 1.935(5) | 1.947(4) | 1.97(2) |
| M(1)–O(5) | 1.905(4) | 1.870(4) | 1.90(2) | M(2)–O(10) | 2.325(1) | 2.320(1) | 2.323(1) |
| M(1)–O(6) | 1.924(6) | 1.888(5) | 1.92(2) | M(3)–O(3) | 1.708(6) | 1.681(5) | 1.67(2) |
| M(1)–O(7) | 1.942(5) | 1.956(5) | 1.97(2) | M(3)–O(6) | 1.929(4) | 1.964(4) | 1.87(2) |
| M(1)–O(10) | 2.325(1) | 2.322(1) | 2.325(1) | M(3)–O(7) | 1.910(3) | 1.890(3) | 1.94(2) |
| M(2)–O(2) | 1.702(4) | 1.669(4) | 1.71(2) | M(3)–O(8) | 1.920(4) | 1.932(4) | 1.90(2) |
| M(2)–O(4) | 1.910(4) | 1.864(3) | 1.95(2) | M(3)–O(9) | 1.917(4) | 1.915(3) | 1.88(2) |
| M(2)–O(5) | 1.933(3) | 1.980(3) | 1.94(2) | M(3)–O(10) | 2.334(1) | 2.310(1) | 2.322(1) |
| O(1)–M(1)–O(4) | 104.0(2) | 102.7(2) | 103.2(9) | O(5)–M(2)–O(8) | 85.8(2) | 84.9(2) | 86.4(8) |
| O(1)–M(1)–O(5) | 103.7(2) | 104.4(2) | 103.5(9) | O(5)–M(2)–O(9) | 86.7(2) | 84.1(2) | 87.1(8) |
| O(1)–M(1)–O(6) | 103.5(2) | 104.1(2) | 105.3(9) | O(5)–M(2)–O(10) | 75.8(2) | 75.5(1) | 76.0(5) |
| O(1)–M(1)–O(7) | 104.1(2) | 102.7(2) | 102.6(9) | O(8)–M(2)–O(9) | 152.3(2) | 152.6(2) | 151.1(7) |
| O(1)–M(1)–O(10) | 180.0(1) | 177.6(1) | 180.0(5) | O(8)–M(2)–O(10) | 76.2(1) | 76.6(1) | 75.4(5) |
| O(4)–M(1)–O(5) | 152.4(2) | 152.7(1) | 153.4(8) | O(9)–M(2)–O(10) | 76.1(1) | 76.3(1) | 75.7(5) |
| O(4)–M(1)–O(6) | 86.2(2) | 85.7(2) | 85.6(7) | O(3)–M(3)–O(6) | 103.2(2) | 102.2(2) | 105.5(9) |
| O(4)–M(1)–O(7) | 86.2(2) | 83.2(2) | 88.3(7) | O(3)–M(3)–O(7) | 104.3(2) | 104.3(2) | 101.1(9) |
| O(4)–M(1)–O(10) | 76.1(1) | 75.4(1) | 76.8(6) | O(3)–M(3)–O(8) | 103.6(2) | 103.4(2) | 104.2(8) |
| O(5)–M(1)–O(6) | 87.5(2) | 90.8(2) | 87.0(7) | O(3)–M(3)–O(9) | 104.1(3) | 103.0(2) | 102.6(8) |
| O(5)–M(1)–O(7) | 87.0(2) | 87.9(2) | 86.4(7) | O(3)–M(3)–O(10) | 179.5(2) | 178.4(1) | 179.0(8) |
| O(5)–M(1)–O(10) | 76.3(1) | 77.5(1) | 76.6(6) | O(6)–M(3)–O(7) | 152.4(2) | 153.5(2) | 153.4(7) |
| O(6)–M(1)–O(7) | 152.4(2) | 152.6(1) | 152.1(8) | O(6)–M(3)–O(8) | 86.2(2) | 85.1(2) | 86.3(7) |
| O(6)–M(1)–O(10) | 76.6(1) | 77.2(1) | 74.7(6) | O(6)–M(3)–O(9) | 86.1(2) | 85.9(1) | 86.6(8) |
| O(7)–M(1)–O(10) | 75.8(1) | 75.8(1) | 77.4(6) | O(6)–M(3)–O(10) | 76.3(2) | 76.1(1) | 75.5(5) |
| O(2)–M(2)–O(4) | 104.0(2) | 104.5(2) | 106.1(9) | O(7)–M(3)–O(8) | 87.1(2) | 87.9(2) | 87.3(7) |
| O(2)–M(2)–O(5) | 103.6(2) | 102.3(2) | 101.7(9) | O(7)–M(3)–O(9) | 87.6(2) | 89.0(1) | 87.7(8) |
| O(2)–M(2)–O(8) | 104.0(2) | 104.0(2) | 104.4(8) | O(7)–M(3)–O(10) | 76.2(2) | 77.3(2) | 77.9(5) |
| O(2)–M(2)–O(9) | 103.7(2) | 102.9(2) | 104.5(8) | O(8)–M(3)–O(9) | 152.3(2) | 153.3(2) | 153.2(7) |
| O(2)–M(2)–O(10) | 179.3(1) | 177.7(1) | 177.8(7) | O(8)–M(3)–O(10) | 76.1(1) | 76.3(1) | 75.9(5) |
| O(4)–M(2)–O(5) | 152.4(2) | 153.1(1) | 152.1(7) | O(9)–M(3)–O(10) | 76.2(2) | 77.1(1) | 77.3(5) |
| O(4)–M(2)–O(8) | 88.2(2) | 90.1(2) | 85.0(7) | | | | |
| O(4)–M(2)–O(9) | 86.2(2) | 88.5(2) | 87.8(7) | | | | |
| O(4)–M(2)–O(10) | 76.6(1) | 77.7(1) | 76.1(5) | | | | |

**Fig. 5** The constituent molecules, atomic numbering, bond lengths (Å) and bond angles (°) for (a) $[tff]_3[W_6O_{19}]$ and (b) $[tff]_3[Mo_6O_{19}]$

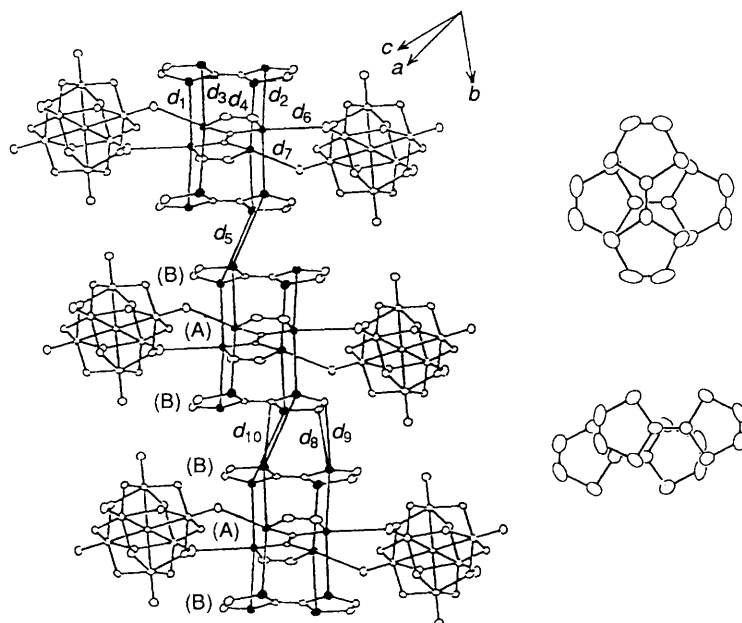


Fig. 6 The ttf stacks in salts **1** and **2** showing the shortest intermolecular contacts (Å): d_1 [$S(1^I) \cdots S(5^I)$] = 3.315(3), 3.304(3); d_2 [$S(1^I) \cdots S(3^{II})$] = 3.528(3), 3.502(3); d_3 [$S(2^I) \cdots S(6^{II})$] = 3.392(3), 3.385(3); d_4 [$S(2^I) \cdots S(4^I)$] = 3.358(3), 3.326(3); d_5 [$S(5^I) \cdots S(6^{III})$] = 4.016(3), 3.999(3); d_6 [$S(2) \cdots O(1)$] = 3.094(4),^v 3.098(4);^{iv} d_7 [$S(1) \cdots O(2)$] = 3.056(5),ⁱⁱⁱ 3.075(3);^{iv} d_8 [$S(4^I) \cdots C(8^{III})$] = 3.55(1), 3.52(1); d_9 [$S(4^I) \cdots C(9^{III})$] = 3.52(1), 3.49(1); d_{10} [$S(5^I) \cdots C(7^{III})$] = 3.57(1), 3.53(1). Symmetry codes: I x, y, z ; II $1-x, 1-y, 1-z$; III $1-x, -y, 1-z$; IV $x, 1+y, z$; V $-x, 1-y, -z$

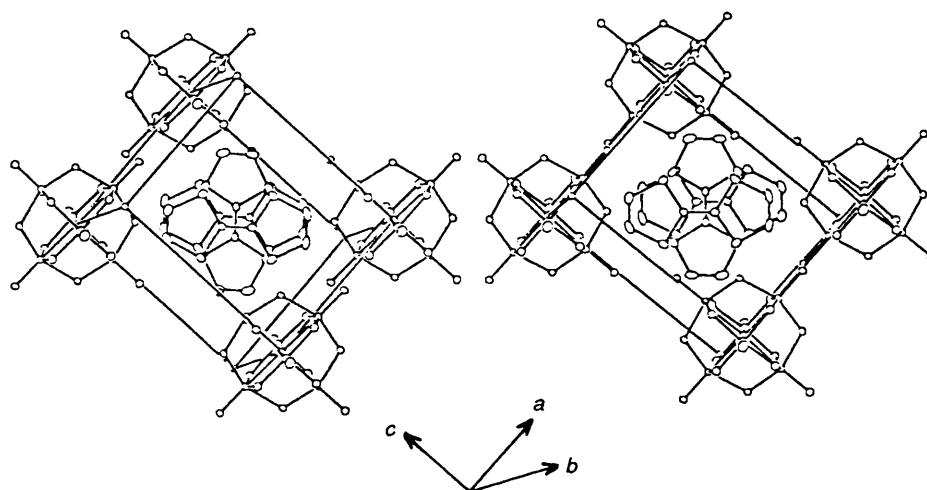


Fig. 7 Stereoscopic view of salts **1** and **2** showing the intratrimer criss-cross overlaps

Table 4 Comparison of averaged bond lengths (Å) in ttf^a

| | 1 | | 2 | | ttf | [ttf][tcnq] | [ttf]ClO ₄ | [ttf] ₃ [BF ₄] ₂ | | [ttf] ₃ [SnCl ₆] | |
|----------|---------------------|--------------------|----------|----------|-----------|--------------------|-----------------------|--|---|---|---|
| | A | B | A | B | | | | A | B | A | B |
| ρ^b | | | | | 0 | +0.59 | +1 | +1 | 0 | + $\frac{2}{3}$ (mean) | |
| <i>a</i> | 1.379(7), 1.353(7) | 1.396(7), 1.383(7) | 1.349(3) | 1.369(4) | 1.404(13) | 1.393(3), 1.347(3) | 1.357(24), 1.360(9) | | | | |
| <i>b</i> | 1.717(5), 1.731(6) | 1.717(5), 1.724(5) | 1.757(2) | 1.743(4) | 1.713(9) | 1.715(2), 1.755(2) | 1.736(10), 1.735(5) | | | | |
| <i>c</i> | 1.725(7), 1.720(8) | 1.711(7), 1.716(7) | 1.726(4) | 1.736(5) | 1.725(12) | 1.719(2), 1.737(2) | 1.717(16), 1.726(6) | | | | |
| <i>d</i> | 1.299(9), 1.324(10) | 1.346(9), 1.33(1) | 1.314(3) | 1.323(4) | 1.306(16) | 1.330(3), 1.322(3) | 1.326(10), 1.345(9) | | | | |
| Ref. | This work | This work | 24 | 25 | 26 | 27 | 28 | | | | |

^a The *mm* symmetry has been imposed. ^b Electronic charge.

C atoms and antibonding between C and S atoms, electron removal from ttf usually results in a lengthening of the C–C bonds and a shortening of the C–S bonds.³¹

The interaction of the HOMOs of the three ttf molecules stacked in a criss-cross fashion leads to the orbital diagram shown in Fig. 9. The HOMO of the inside ttf molecule (A) of

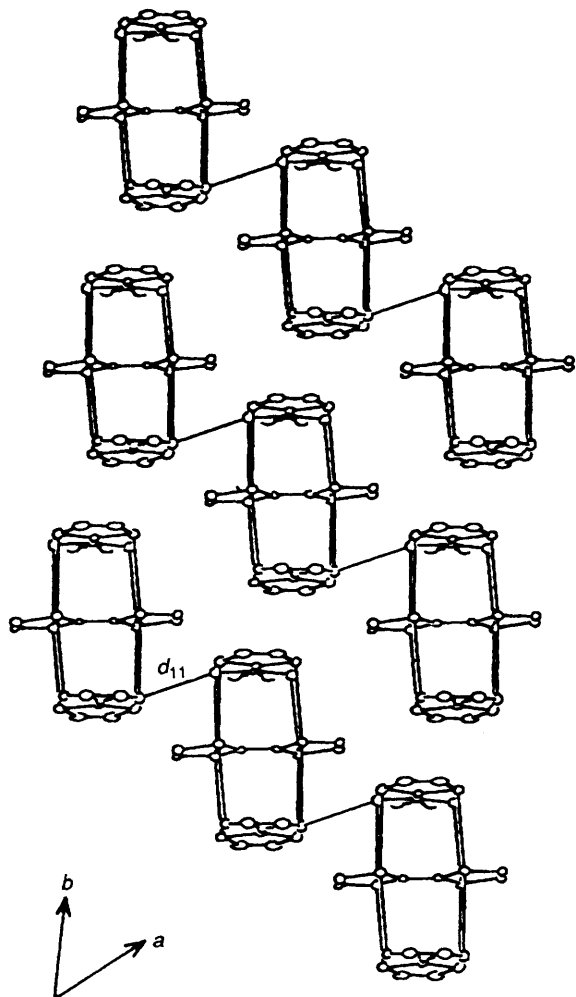


Fig. 8 Projection of the structures of salts **1** and **2** onto the ab plane, showing the interstack $S \cdots S$ contacts: d_{11} [$S(3) \cdots S(3')$] = 3.430(2) and 3.415(2) Å for **1** and **2** respectively; $1 - x, 1 - y, 1 - z$

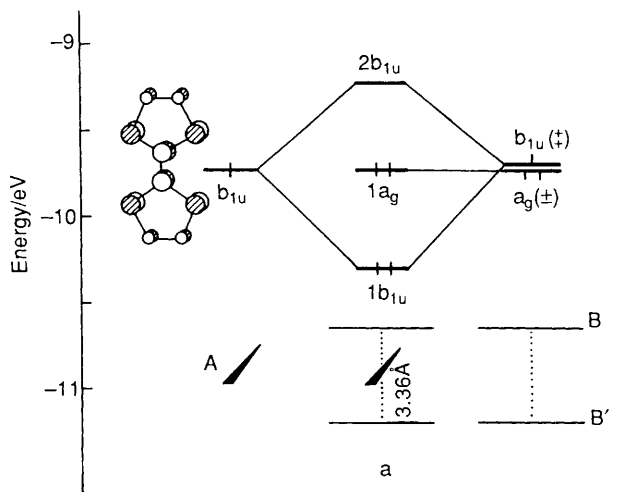


Fig. 9 Interaction diagram of the HOMOs of three ttf molecules

b_{1u} symmetry interacts with the in-phase combination of the HOMOs of the two outside molecules (B and B') of the same symmetry. The out-of-phase combination of a_g symmetry remains unperturbed after interaction. With a four-electron system in a low-spin state, the mixed-valence $ttf^{\pm\pm}$, ttf^+ , $ttf^{\pm\pm}$ structure is straightforward. With two bonding and two non-

bonding electrons, the situation is reminiscent of what is encountered with a linear H_3^- molecule.³³ Note that the same situation would prevail if the three ttf molecules were eclipsed as in $[tft]_3[SnCl_6]^{28}$ because of the local D_{2h} symmetry, *i.e.* the presence of an inversion centre on the inside ttf molecule. A change in the electronic distribution would occur with a high-spin state. We do not envisage this situation here since compounds **1** and **2** are diamagnetic materials.

A glance at the overlap populations between atoms in the triad **a** (BAB), shown in Scheme 2, indicates that the asymmetric electronic distribution induces some differences between the bonds of the outside molecules and the corresponding ones of the inside molecule. For instance, the central C–C overlap population is 1.11 for molecule A, somewhat weaker than the 1.17, computed for the corresponding bond in molecules B and B'. On the other hand, the C–S overlap populations are slightly larger in the inside molecule than in the outside ones. Consequently, this difference in bond strengths might lead to different bond distances,³³ in accord with the observed distances in **1** and **2**. Though less pronounced in **2** than in **1**, the central C–C bond is longer in ttf A than in B and B', while the average C–S bonds are slightly shorter (see above).

Tight-binding calculations on the two-dimensional donor sublattice of compound **1** confirm the assigned mixed-valence structure. Charges of 1.12+ and 0.44+ are computed for the A and B ttf molecules respectively. The shift of the charges compared to those obtained for model **a** is mainly due to intramolecular structural relaxation observed in **1**. The HOMO of the A ttf is no longer degenerate with the HOMOs of the B and B' ttf, but slightly higher in energy.³¹ Consequently, the occupied bonding combination ($1b_{1u}$ MO in **a**) becomes more localized on the B and B' ttf molecules, leading to reduction of the positive charge, while the reverse happens for molecule A.

The bands derived from the HOMOs of the ttf triads are shown in Fig. 10(a). The $\Gamma \rightarrow X$ direction and the $\Gamma \rightarrow Y$ direction in reciprocal space correspond to the inter-stack coupling a axis and the stacking b axis respectively. Though there are some relatively short non-bonding $S \cdots S$ interstack contacts of 3.43 Å in the a direction (d_{11} in Fig. 8), the bands are nearly flat along the $\Gamma \rightarrow X$ direction. This reflects negligible interstack interactions. The weak band dispersion comes from the fact that the interstack $S \cdots S$ overlap along that direction is essentially π in nature and therefore not very important. This is not the case along the $\Gamma \rightarrow Y$ direction where some band dispersion is noted due to intertrimer interactions between sulfur and carbon atoms which overlap in a more or less σ fashion (see $S \cdots C$ contacts in Fig. 6). We conclude that salts **1** and **2** present quasi-one-dimensional band structures with a narrow band width ($\Delta \leq 0.5$ eV).

The band gap of about 0.45 eV calculated for the organic slabs of salt **1** is in agreement with the semiconducting properties of compounds **1** and **2**.

IR absorption bands. The criss-cross trimer arrangement in the crystal structure of the ttf salts **1** and **2** is a particular and unusual case of centrosymmetrical trimers which has not yet been considered theoretically. When the electron-molecular vibration linear coupling is introduced, it gives rise to the classical vibronic mode.^{34a} The only example known so far is $[tmtsf]_3[PW_{12}O_{40}]$ which is an insulator.³ In the spectrum of this salt there is only a c.t. 'B' band and a relatively weak vibronic band at around 1340 cm^{-1} , the frequency of which is almost unchanged with temperature.^{34b} The existence of a vibronic band for a criss-cross trimer proves that electron-molecular vibration coupling is allowed in the present situation.

Indeed for our ttf salts **1** and **2** the vibronic band is observed at around 1380 cm^{-1} . This frequency and the associated 'A' band are the same as those observed in the case of perpendicular trimers such as $[tft]_4[MCl_4]_4$ ($M = Mn$ or Co)¹⁷ for which no temperature dependence of the vibronic band is observed. In the present situation a weak temperature

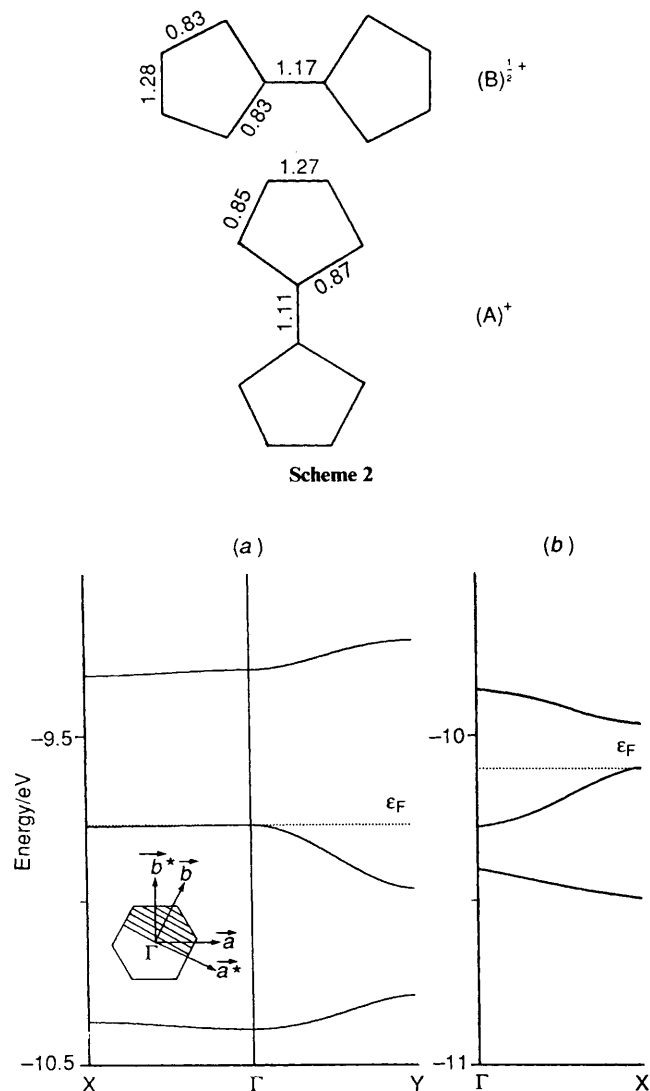


Fig. 10 Electronic band structure for (a) the $(\text{ttf})_3^{2+}$ slabs in $[\text{tft}]_3[\text{W}_6\text{O}_{19}]$ (the Brillouin zone is shown in the inset) and (b) the $(\text{tmtsf})_3^{2+}$ chain in $[\text{tmtsf}]_3[\text{W}_6\text{O}_{19}] \cdot 2\text{dmf}$

dependence is observed [see Fig. 4(b)] which could be attributed either to some molecular charge in the trimer because of a strong thermal dilatation, or to a modification of the electron-molecular vibration coupling due to a different behaviour of the c.t. bands. In the absence of any experimental data at low temperature we are unable to confirm or reject this last hypothesis.

$[\text{tmtsf}]_3[\text{W}_6\text{O}_{19}] \cdot 2\text{dmf}$ 3.—*Crystal structure.* The bond distances and angles are given in Fig. 11 for the tmtsf molecules of $[\text{tmtsf}]_3[\text{W}_6\text{O}_{19}] \cdot 2\text{dmf}$ 3. The crystal structure shown in Figs. 12 and 13 is built from $\text{W}_6\text{O}_{19}^{2-}$ anions located at the origin of the lattice, and two independent tmtsf units denoted A and B: molecule A is centred on the $(0,0,\frac{1}{2})$ inversion centre and B in general position. The molecules of solvent (dmf) are located in the middle of the unit cell.

The bond distances of the two independent tmtsf molecules are averaged in the *mm* symmetry and compared in Table 5 with the corresponding distances encountered in other tmtsf^{x+} salts ($x = 0$ or 1).^{16,35b,37} These bond distances compare rather well with those observed in other 3:1 salts, especially with $[\text{tmtsf}]_3[\text{Pt}(\text{CN})_4]$.¹⁶ The tmtsf molecules form trimerized and slipped stacks (Fig. 13) parallel to the $[100]$ direction. The spacing between adjacent tmtsf molecules inside a trimer (3.53

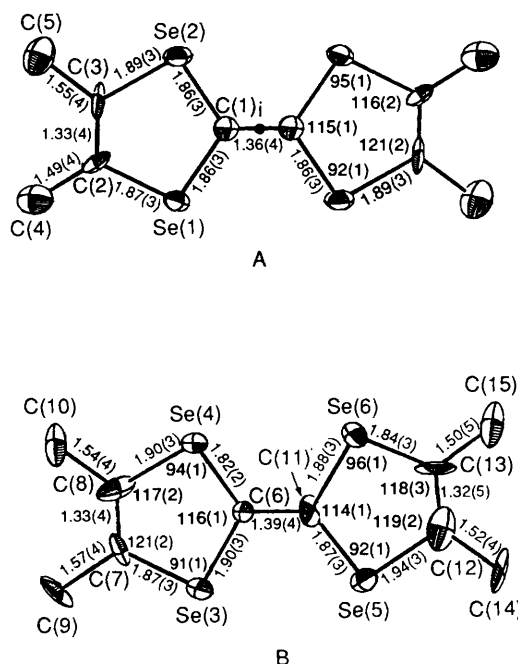


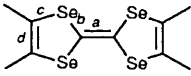
Fig. 11 The constituent molecules, atomic numbering, bond lengths (Å) and bond angles ($^\circ$) for $[\text{tmtsf}]_3[\text{W}_6\text{O}_{19}] \cdot 2\text{dmf}$

and 3.63 Å) and the intra- and inter-trimer ring-over-central bond overlaps (Fig. 12) are comparable to those found in other tmtsf salts.³⁵ This mode of overlap generates in the present compound slipped stacks similar to that observed in the black phase of $[\text{tmtsf}][\text{tcnq}]$ (tcnq = tetracyanoquinodimethane),³⁶ in contrast with the zigzag ones observed commonly in the $[(\text{tmtsf})_2]^+ \text{X}^-$ ($\text{X} = \text{PF}_6$ or BF_4) series³⁵ or in other $[(\text{tmtsf})_3]^{2+} \text{X}^{2-}$ [$\text{X} = \text{Pt}(\text{CN})_4$ or $\text{Ni}(\text{CN})_4$] compounds.¹⁶ The intra-trimer Se...Se contacts range between 3.73 and 3.81 Å (Fig. 13). They are shorter than those commonly observed in the 2:1 salts.³⁵ The inter-trimer Se...Se contacts (3.94–4.12 Å) are in the range of the corresponding van der Waals separations (4 Å). Short O...Se anion-cation interactions are also observed: Se(6)...O(3) 3.17(2), Se(4)...O(2) 3.21(2) and Se(1)...O(7) 3.21(2) Å (van der Waals distance: 3.4 Å).

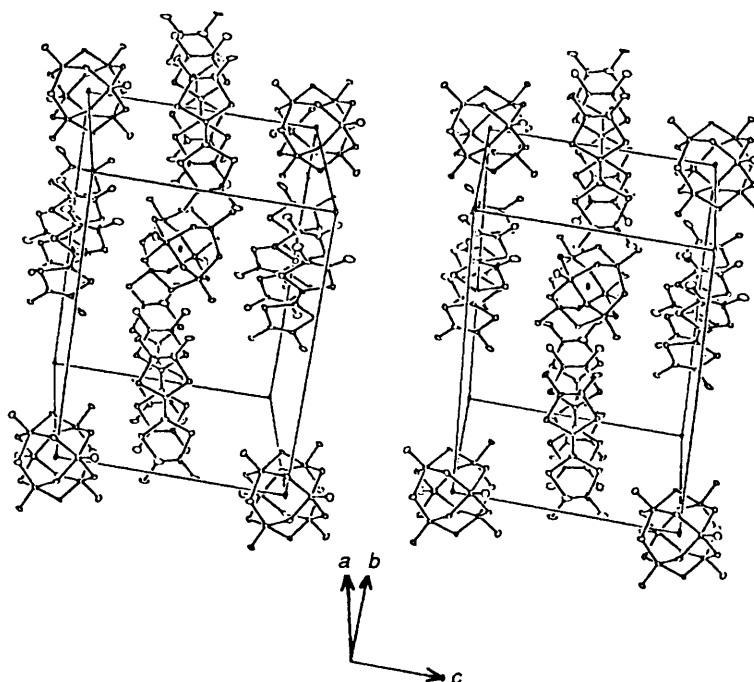
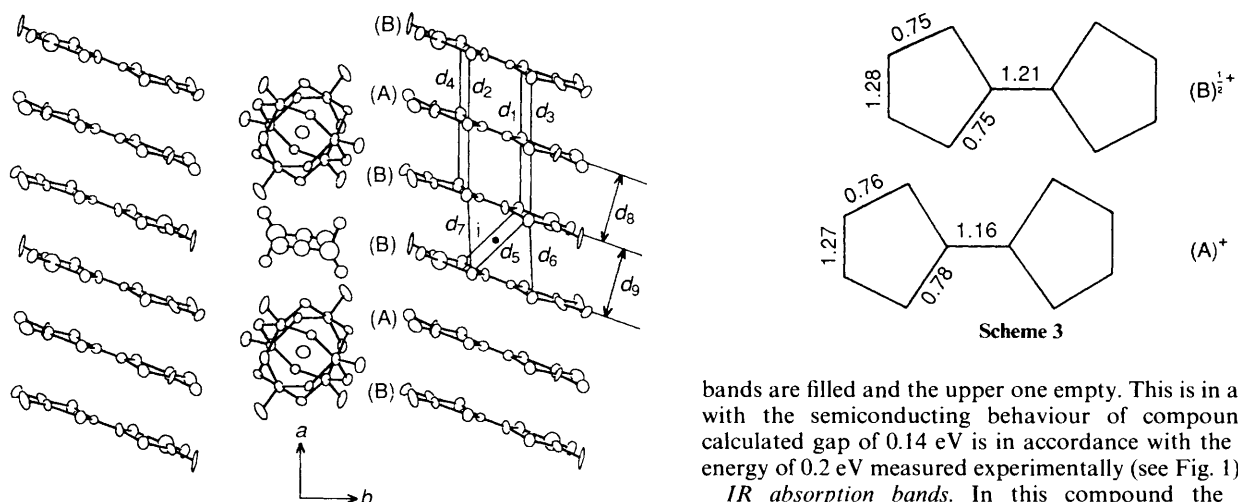
Theoretical band calculations. As in compounds 1 and 2, a mixed-valence structure is computed for the $(\text{tmtsf})_3^{2+}$ stack present in 3. Molecular calculations on the $(\text{tmtsf})_3^{2+}$ triad **b** made of two 'outside' tmtsf molecules B and B' and one 'inside' molecule A, give the $\text{tmtsf}^{\pm+}$, tmtsf^+ , $\text{tmtsf}^{\pm+}$ charge sequence. Here again the unsymmetrical electron distribution is due to the presence of an inversion centre located on the A molecule. With identical separations for both inside and outside tmtsf molecules (central C–C, C–Se and edge C–C bond distances of 1.35, 1.90 and 1.33 Å respectively), the overlap populations between different atoms shown in Scheme 3 indicate that a weak intramolecular structural relaxation might occur.³¹ Bond distances determined by X-ray crystallography are not accurate enough to reveal this structural deformation.³¹

In agreement with the molecular calculations, a mixed-valence $\text{tmtsf}^{0.54+}$, $\text{tmtsf}^{0.92+}$, $\text{tmtsf}^{0.54+}$ structure is obtained from tight-binding calculations on the one-dimensional chain of $(\text{tmtsf})_3^{2+}$ triads encountered in salt 3. Combinations of the HOMOs of the three tmtsf molecules constituting each trimer lead to three molecular orbitals (one bonding, one non-bonding and one antibonding) which mainly comprise the three bands shown in Fig. 10(b). The band dispersion which is observed translates some intertrimer interactions predominantly through σ overlap between Se atoms separated by 3.94 Å (d^5 contacts in Fig. 13). Nearly zero but positive overlap population is computed between these Se atoms.

With a formal oxidation state of $(\text{tmtsf})_3^{2+}$, the two lower

Table 5 Comparison of averaged bond lengths (Å) in tmtsf*


| | A | B | tmtsf | [tmtsf] ₂ PF ₆ ⁻ | [tmtsf] ₃ [Pt(CN) ₄] |
|----------|-----------|---------|----------|---|---|
| <i>a</i> | 1.36(4) | 1.39(4) | 1.35(1) | 1.369(14) | 1.352(11), 1.373(11) |
| <i>b</i> | 1.86(3) | 1.87(3) | 1.892(7) | 1.875(10) | 1.878(8), 1.859(8) |
| <i>c</i> | 1.88(3) | 1.89(3) | 1.906(7) | 1.893(10) | 1.901(8), 1.887(8) |
| <i>d</i> | 1.33(4) | 1.32(4) | 1.32 | 1.329(15) | 1.323(12), 1.346(11) |
| Ref. | This work | | 37 | 35(b) | 16 |

* The *mmm* symmetry has been imposed.**Fig. 12** Stereoscopic view of the structure of salt 3 showing the intermolecular overlaps**Fig. 13** Side view of the tmtsf stack showing shortest intra- and inter-trimer contacts (Å): d_1 [Se(1^I)...Se(3^I)] = 3.753(5), d_2 [Se(1^I)...Se(6^{II})] = 3.731(5), d_3 [Se(2^I)...Se(4^I)] = 3.745(5), d_4 [Se(2^I)...Se(5^{II})] = 3.807(5), d_5 [Se(5^I)...Se(6^{III})] = 3.940(4), d_6 [Se(4^I)...Se(5^{III})] = 4.047(5), d_7 [Se(3^I)...Se(6^{III})] = 4.120(5), d_8 = 3.53, d_9 = 3.63. Symmetry codes: I *x*, *y*, *z*; II $-x$, $-y$, $1-z$; III $1-x$, $-y$, $1-z$

bands are filled and the upper one empty. This is in accordance with the semiconducting behaviour of compound 3. The calculated gap of 0.14 eV is in accordance with the activation energy of 0.2 eV measured experimentally (see Fig. 1).

IR absorption bands. In this compound the molecular arrangement of the trimers is very similar to that encountered in [(tmtsf)₃][M(CN)₄] (M = Pt or Ni) salts.¹⁶ The electronic 'A' band and the vibronic mode are observed at about the same energy. The c.t. 'B' band (Fig. 2) can be related to the hopping of charges towards the oxidized molecule in order to get a double occupancy.

Conclusion

Using the standard electrocrystallization technique, we have obtained new 3:1 salts of ttf and tmtsf with Lindquist-type W_6O_{19} and Mo_6O_{19} dianions. These salts show one-dimensional trimerized organic stacks with both unusual criss-cross and ring-over-double bond intratrimer overlaps in the ttf and tmtsf salts respectively. Mixed-valence ($\frac{1}{2}+$, $1+$, $\frac{1}{2}+$) structures for the organic donor trimers are determined on the basis of their bond lengths and electronic band-structure calculations. The three compounds are diamagnetic semiconductors: this semiconducting behaviour associated with a localized mixed-valence state in these salts is confirmed by the spectra which show rather classical vibronic modes induced by two charge-transfer bands. These results are in agreement with the Robin–Day classification³⁸ which is based on the degree of π charge transfer associated with each site. Organic conductors which present a metallic or even a supraconducting state belong to class III where the mean degree of charge transfer is homogeneous (or constant), whereas the present salts exhibit a localized mixed-valence behaviour as in class II. This largely confirms that the same classification can be used for both organic and inorganic compounds.

Acknowledgements

Thanks are expressed to A. Flattet and C. Hervieu for their technical assistance in electrochemical experiments and L. Hubert for the illustrations.

References

- L. Ouahab, M. Bencharif and D. Grandjean, *C. R. Acad. Sci., Ser. 2*, 1988, **307**, 749.
- (a) S. Triki, L. Ouahab, J. Padiou and D. Grandjean, *J. Chem. Soc., Chem. Commun.*, 1989, 1068; (b) C. Bellito, D. Attanzio, M. Bonamico, V. Fares, P. Imperatori and S. Patrizio, *Mater. Res. Soc. Proc.*, 1990, **173**, 143.
- (a) L. Ouahab, S. Triki, D. Grandjean, M. Bencharif, C. Garrigou-Lagrange and P. Delhaes, *Lower-dimensional Systems and Molecular Electronics*, eds. R. M. Metzger, P. Day and G. C. Papavassiliou, NATO ASI Series, Plenum, New York, 1991, **B248**, 185; (b) S. Triki, L. Ouahab, D. Grandjean, J. Amiel, C. Garrigou-Lagrange, P. Delhaes and J. M. Fabre, *Synth. Met.*, 1991, **41–43**, 2589; (c) A. Mhanni, L. Ouahab, O. Peña, D. Grandjean, C. Garrigou-Lagrange and P. Delhaes, *Synth. Met.*, 1991, **41–43**, 1703.
- (a) I. Lindquist, *Ark. Kemi*, 1953, **5**, 247; (b) J. F. Keggin, *Proc. R. Soc. London, Ser. A*, 1934, **144**, 75.
- M. T. Pope, in *Heteropoly and Isopoly Oxometalates*, Springer, New York, 1983; M. T. Pope and G. M. Varga, *Inorg. Chem.*, 1966, **5**, 1249; M. T. Pope and E. Papaconstantinou, *Inorg. Chem.*, 1967, **6**, 1147; G. M. Varga, E. Papaconstantinou and M. T. Pope, *Inorg. Chem.*, 1970, **9**, 662; (e) J. P. Launay, *J. Inorg. Nucl. Chem.*, 1976, **18**, 807; C. L. Hill, D. A. Bouchard, M. Kadkhodayan, M. M. Williamson, J. A. Schmidt and E. F. Hilinsky, *J. Am. Chem. Soc.*, 1988, **110**, 5471 and refs. therein; M. T. Pope and A. Muller, *Angew. Chem., Int. Ed. Engl.*, 1991, **30**, 34.
- M. Che, M. Fournier and J. P. Launay, *J. Chem. Phys.*, 1979, **71**, 1954.
- C. Sanchez, J. Livage, J. P. Launay and M. Fournier, *J. Am. Chem. Soc.*, 1983, **105**, 6817.
- (a) A. C. T. North, D. C. Phillips and F. S. Mathews, *Acta Crystallogr., Sect. A*, 1968, **24**, 351; (b) N. Walker and D. Stuart, *Acta Crystallogr., Sect. A*, 1983, **39**, 158.
- P. Main, S. J. Fiske, S. E. Hull, L. Lessinger, G. Germain, J. P. Declercq and M. M. Woolfson, MULTAN 84, A system of computer programs for the automatic solution of crystal structures from X-ray diffraction data, Universities of York and Louvain, 1984.
- International Tables for X-Ray Crystallography*, Kynoch Press, Birmingham (present distributor, D. Reidel, Dordrecht), 1974, vol. 4.
- C. K. Johnson, ORTEP, Report ORNL-3794, Oak Ridge National Laboratory, Oak Ridge, TN, 1965.
- B. A. Frenz and Associates, SDP Structure Determination Package, College Station, TX, and Enraf-Nonius, Delft, 1985.
- J. B. Torrance, B. A. Scott and F. B. Kaufman, *Solid State Commun.*, 1975, **17**, 1369.
- C. Garrigou-Lagrange, P. Delhaes, L. Ouahab and P. Batail, *Dynamics of Molecular Crystals*, ed. J. Lascombe, Elsevier, Amsterdam, 1987, p. 287.
- C. Garrigou-Lagrange, L. Ouahab, D. Grandjean and P. Delhaes, *Synth. Met.*, 1990, **35**, 9.
- L. Ouahab, J. Padiou, D. Grandjean, C. Garrigou-Lagrange, P. Delhaes and M. Bencharif, *J. Chem. Soc., Chem. Commun.*, 1989, 1038.
- G. Maceno, C. Garrigou-Lagrange, P. Delhaes, F. Bechtel, G. Bravic, J. Gaultier, M. Lequan and R. M. Lequan, *Synth. Met.*, 1988, **27**, B57.
- C. Rocchiccioli-Deltcheff, M. Fournier, R. Franck and R. Thouvenot, *J. Mol. Struct.*, 1984, **114**, 49.
- M.-H. Whangbo and R. Hoffmann, *J. Am. Chem. Soc.*, 1978, **100**, 6093; M.-H. Whangbo, R. Hoffmann and R. B. Woodward, *Proc. R. Soc. London, Ser. A*, 1979, **366**, 23.
- R. Hoffmann, *J. Chem. Phys.*, 1962, **39**, 1397.
- R. Ramirez and M. C. Böhm, *Int. J. Quantum Chem.*, 1986, **30**, 391.
- (a) V. J. Fuchs, W. Freiwald and H. Hartl, *Acta Crystallogr., Sect. B*, 1978, **34**, 1764; (b) R. Bhattacharyya, S. Biswas, J. Armstrong and E. M. Hott, *Inorg. Chem.*, 1989, **28**, 4297.
- (a) H. R. Allcock, E. C. Bissel and E. T. Shawl, *Inorg. Chem.*, 1973, **12**, 2963; (b) W. Clegg, G. M. Sheldrick, C. D. Garner and I. B. Walton, *Acta Crystallogr., Sect. B*, 1982, **38**, 2906 and refs. therein.
- W. F. Cooper, N. C. Kenny, J. W. Edmonds, A. Nagel, F. Wudl and P. Coppens, *Chem. Commun.*, 1971, 889.
- T. J. Kistenmacher, T. E. Phillips and D. O. Cowan, *Acta Crystallogr., Sect. B*, 1974, **30**, 763.
- K. Yakushi, S. Nishimura, T. Sugano and H. Kuroda, *Acta Crystallogr., Sect. B*, 1980, **36**, 358.
- J. P. Legros, M. Bousseau, L. Valade and P. Cassoux, *Mol. Cryst. Liq. Cryst.*, 1983, **100**, 181.
- K. Kondo, G. Matsubayashi, T. Tanaka, H. Yoshioka and K. Nakatsu, *J. Chem. Soc., Dalton Trans.*, 1984, 379.
- P. Batail, L. Ouahab, J. B. Torrance, M. L. Pylman and S. S. P. Parkin, *Solid State Commun.*, 1985, **55**, 597.
- H. Kobayashi, A. Kobayashi, Y. Sasaki, G. Saito and H. Inokuchi, *Bull. Chem. Soc. Jpn.*, 1983, **56**, 2894.
- S. S. Shaik and M.-H. Whangbo, *Inorg. Chem.*, 1986, **25**, 1201.
- J. P. Lowe, *J. Am. Chem. Soc.*, 1980, **102**, 1262.
- T. A. Albright, J. K. Burdett and M.-H. Whangbo, in *Orbital Interactions in Chemistry*, Wiley, New York, 1985.
- (a) C. Garrigou-Lagrange, unpublished work; (b) V. M. Yartsev, *Phys. States Solidi. B*, 1982, **112**, 279.
- (a) K. Bechgaard, S. Jacobsen, K. Mortensen, H. J. Pedersen and N. Thorup, *Solid State Commun.*, 1980, **33**, 1119; (b) N. Thorup, G. Rindorf, H. Soling and K. Bechgaard, *Acta Crystallogr., Sect. B*, 1981, **37**, 1236; (c) J. M. Williams, M. A. Beno, H. H. Wang, P. C. W. Leung, T. J. Emge, U. Geiser and K. D. Carlson, *Acc. Chem. Res.*, 1985, **18**, 261; (d) J. M. Williams, *Prog. Inorg. Chem.*, 1985, **33**, 183, and refs. therein; (e) J. M. Williams, M. A. Beno, E. H. Appelman, J. M. Capriotti, F. Wudl, E. Aharon-Sharon and D. Nalewajek, *Mol. Cryst. Liq. Cryst.*, 1982, **79**, 319.
- K. Bechgaard, J. T. Kistenmacher, A. N. Bloch and D. O. Cowan, *Acta Crystallogr., Sect. B*, 1977, **33**, 417.
- T. J. Kistenmacher, T. J. Emge, P. Shu and D. O. Cowan, *Acta Crystallogr., Sect. B*, 1979, **35**, 772.
- M. B. Robin and P. Day, *Adv. Inorg. Chem. Radiochem.*, 1967, **10**, 247.

Received 7th October 1991; Paper 1/05099K